

Section 9

**Development of and studies with
coupled ocean-atmosphere models**

Update of the JMA's El Niño Prediction System in February 2009

Masayuki Hirai¹, Ichiro Ishikawa¹, Akihiko Shimpo¹, Taizo Soga¹, Hirotohi Mori¹,
Yosuke Fujii², Satoshi Matsumoto² and Tamaki Yasuda²

¹ Climate Prediction Division, Japan Meteorological Agency, Tokyo, Japan

² Oceanographic research Department, Meteorological Research Institute, Tsukuba, Japan
(E-mail: m-hirai @ met.kishou.go.jp)

1. Introduction

In February 2009, JMA updated the El Niño prediction system, which consists of a global ocean data assimilation system (MOVE/MRI.COM-G; Usui et al. 2006) and a coupled atmosphere-ocean global circulation model (JMA/MRI-CGCM; Takaya et al. 2007). The operational information, such as the El Niño outlook¹ and monitoring of global oceanic condition², has been produced with the new system since March 2009. This paper reports the overview of the update and the prediction skill by the hindcast experiments.

2. Outline of the JMA's El Niño prediction system

Specifications of the JMA/MRI-CGCM are shown in Table 1. The atmospheric component is a lower-resolution version of the global spectral model (GSM0603) used by JMA for operational numerical weather prediction (JMA, 2007). The atmospheric initial conditions are referred to the climate data assimilation system in JMA (JCDAS). The oceanic initial conditions are provided by the ocean data assimilation system (MOVE/MRI.COM-G), which adopts multivariate three dimensional variational (3D-VAR) method with vertical coupled Temperature-Salinity (T-S) Empirical Orthogonal Function (EOF) modes. Coupling of heat, momentum and fresh water flux between the oceanic and atmospheric components takes every one-hour. In order to mitigate climate drift, flux adjustment of both heat and momentum flux are given during time integration.

3. Major changes of this update

The oceanic perturbation has been newly implemented in the new system. The oceanic perturbed initial members are estimated through the ocean data assimilation system forced with the perturbed surface wind stress fields, which are produced by the atmosphere breeding method. Therefore, the ensemble method has been improved as follows (Figure 1);

(Old) Lagged Average Forecasting (LAF) ensemble
(one member with twelve initial dates)

(New) Combination of perturbations and LAF
ensemble (five members with six initial dates)

Accordingly, ensemble size has been increased from 12

to 30 and the lag period has been shortened from 55 to 25 days.

In addition, some statistics, such as the T-S EOF modes for MOVE/MRI.COM-G, flux adjustment and bias correction of SSTs for JMA/MRI-CGCM have been replaced according to the improvement of the MOVE/MRI.COM-G.

4. Performance

To examine the impacts of refining the ensemble method, the performances of the following two ensemble methods were compared in a hindcast experiment (Figure 2);

LAF5: A 10-day LAF ensemble consisting of five members

PTB10: A combination of the 25-day LAF ensemble and perturbations consisting of 10 members

Four initial dates per year were set for the experiment (31 January, 1 May, 30 July and 28 October) for the period from spring 1996 to spring 2006 (10 years). The ensemble size of **PTB10** was larger than that of **LAF5**, and the lag period for **PTB10** was shorter than that of **LAF5**. It can be estimated that the difference in performance of both methods corresponds approximately to the improvement in forecast skills brought about by this upgrade.

It is found that **PTB10** improves on the prediction of SSTs over the western tropical Pacific and the Indian Ocean (Figure 3). This improvement can mainly be attributed to the increased ensemble size compared with the result of other methods in aggregating ensemble members (not shown). Perturbations used in the new ensemble method are important to increase ensemble size within a limited time.

References

- Yasuda, T., Y. Takaya, C. Kobayashi, M. Kamachi, H. Kamahori, and T. Ose, 2007: Asian monsoon predictability in JMA/MRI seasonal forecast system. CLIVAR Exchange, 43, 18-24.
- Usui, N., S. Ishizaki, Y. Fujii, H. Tsujino, T. Yasuda and M. Kamachi, 2006: Meteorological Research Institute multivariate ocean variational estimation (MOVE) system. Advances in Space Research, 37, 806-822.
- Takaya, Y., T. Yasuda, S. Matsumoto, T. Nakaegawa and T. Ose, 2007: Seasonal Prediction Skill in the New ENSO Forecast System at Japan Meteorological Agency. WCRP Workshop on Seasonal Prediction, Barcelona Spain June 4-7, 2007.

¹ <http://ds.data.jma.go.jp/tcc/tcc/products/elnino/index.html>

² <http://ds.data.jma.go.jp/tcc/tcc/products/clisys/index.html>

Table 1 Specifications of the El Niño prediction model (JMA/MRI-CGCM)

Atmospheric component	Domain	Global
	Resolution	TL95, 40 vertical levels
Oceanic component	Domain	Global except the Arctic Ocean (75°S-75°N)
	Resolution	1.0° (long.) x 1.0° (lat.), (1.0° (long.) x 0.3° (lat.) near equator) 50 vertical levels
Coupling	Frequency	Every one-hour
	Flux adjustment	heat and momentum fluxes

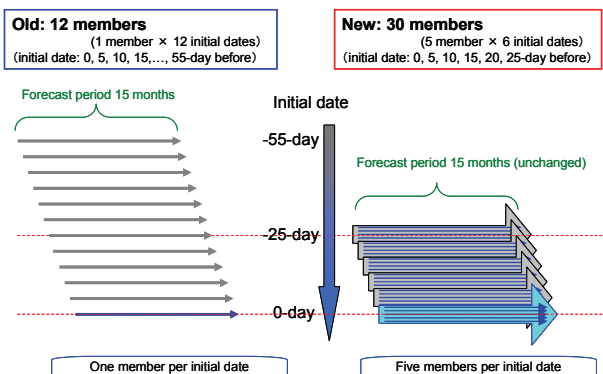


Figure 1 Schema of the aggregation of ensemble members in the old (left) and new (right) El Niño prediction system.

PTB10 vs. LAF5

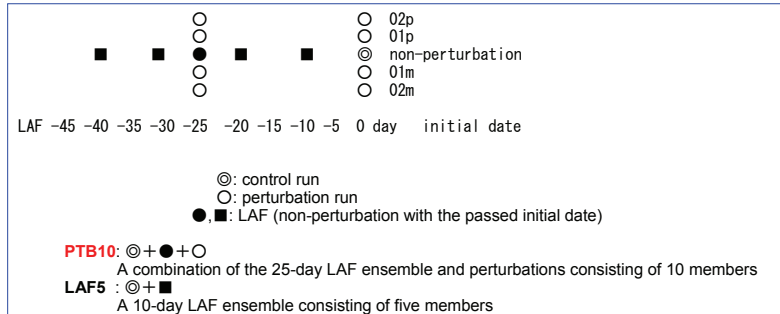


Figure 2 Schema of two ensemble methods (PTB10 and LAF5) in the hindcast experiment.

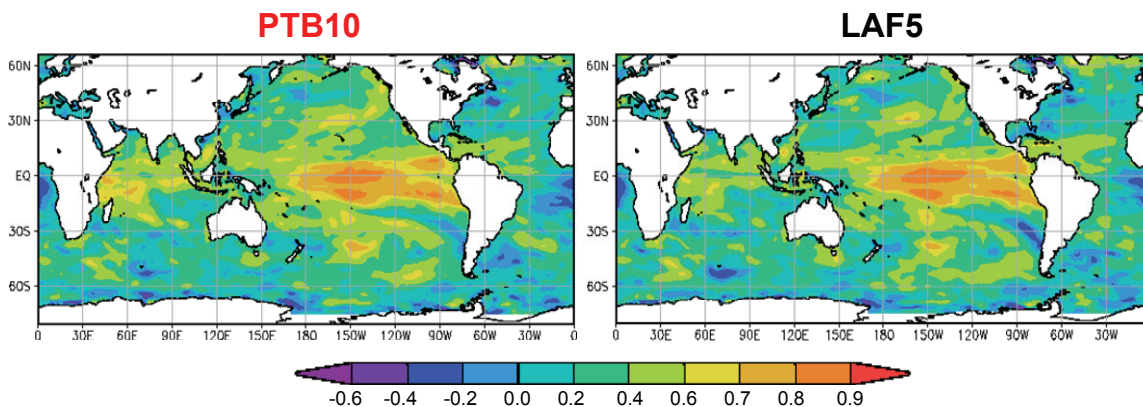


Figure 3 Anomaly correlation coefficient of SST prediction by PTB10 (left) and LAF5 (right) Lead time is six months.

Design and first simulation with a tri-coupled AORCM dedicated to the Mediterranean study

Samuel Somot, Florence Sevault and Michel Déqué
Centre National de Recherches Météorologiques, Météo-France.
42 avenue Coriolis F-31057 Toulouse Cedex, France, samuel.somot@meteo.fr

The Mediterranean Sea can be considered as a thermodynamic machine that exchanges water and heat with the Atlantic Ocean through the Strait of Gibraltar and with the atmosphere through its surface. Considering the Mediterranean Sea Water Budget (MSWB) multi-year mean, the Mediterranean basin loses water by its surface with an excess of the evaporation over the freshwater input (precipitation, river runoff, Black Sea input). Moreover the MSWB largely drives the Mediterranean Sea water mass formation and therefore a large part of its thermohaline circulation. This could even have an impact on the characteristics of the Atlantic thermohaline circulation through the Mediterranean Outflow Waters (MOW) that flow into the Atlantic at a depth of about 1000 m. From a climate point of view, the MSWB acts as a water source for the Mediterranean countries and then plays an important role on the water resources of the region. Consequently the Mediterranean basin can impact the global climate through two branches, the fast atmospheric branch through the regional air-sea interactions and the water vapour transport and the slow oceanic branch through the Mediterranean deep water masses, the MOW and the Atlantic Ocean thermohaline circulation.

To represent the impact of the Mediterranean basin on the global climate, we must at least accurately simulate the MSWB that drives the fast branch as well as the formation of the Mediterranean deep water masses that lead to the MOW. This requires to work with both high resolution atmosphere models and high resolution ocean models. This is mainly due to the complexity of the topography surrounding the Mediterranean basin, as well as the complexity of the Mediterranean sub-basins and straits, its air-sea fluxes and its water mass system. Moreover we must also simulate the feedbacks of the MSWB and of the MOW on the global coupled climate system that is to say the branches themselves.

Pursuing that goal we decided to develop a Mediterranean high-resolution Atmosphere-Ocean Regional Climate Model (AORCM) embedded in a global coupled model. This new numerical tool should allow to address the following scientific issues:

- What is the full climate variability of the Gibraltar Strait exchanges ?
- How does it affect the Mediterranean air-sea fluxes variability ?
- What is the full climate variability of the MOW ?
- What is the impact of the MOW on the Atlantic thermohaline circulation and then on the global climate ?
- What is the impact of the water vapor transport from the Mediterranean area on the global climate ?

Technically speaking, we created a tri-coupled model coupling the stretched-grid ARPEGE-Climate model (Déqué and Piedelievre 1995) with two ocean models, the global NEMO-ORCA2 (Madec, 2008) and the Mediterranean NEMO-MED8 (Somot et al. 2006, Sevault et al. 2009).

The ARPEGE-Climate atmosphere model is used here in its version 4.6 for the physics www.cnrm.meteo.fr/gmcec/site_engl/arpege/arpege_en.html and with the *mediash* configuration (TL159c2.5, 31 vertical levels). This particular configuration covers the whole planet with a stretched grid allowing a refinement over the Mediterranean area (see Figure 1a) with a spatial resolution of about 50 km over the area of interest. The stretched version of ARPEGE-Climate has already been coupled to a Mediterranean Sea ocean model (Somot et al. 2008).

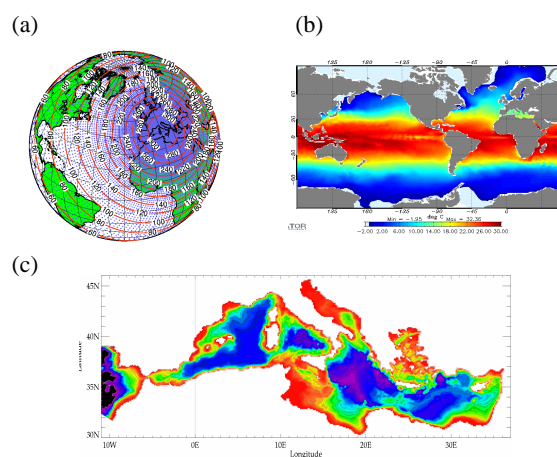


Figure 1: Domain and grid definition of (a) the stretched ARPEGE-Climate, (b) the global NEMO-ORCA2 ocean model and (c) the NEMO-MED8 regional ocean model.

The global ocean is a global version of the NEMOv2 ocean platform in which the ocean model is based on OPA9 (Madec 2008). The horizontal mesh is based on a 2° by 2° Mercator grid (i.e., same zonal and meridional grid spacing). The ORCA2 grid (see Figure 1b) is used in this study in which the resolution evolves from 0.5° in the tropics to 2° close to the poles. The resolution is about 1° at the latitude of the Mediterranean Sea. There are 31 levels in the vertical, with the highest resolution (10 m) in the upper 150 m. This version of the model is developed at LOCEAN with modification mainly concerning the ocean-atmosphere coupling done at CERFACS.

The NEMO-MED8 model is a Mediterranean version of the same NEMOv2 platform developed at CNRM. The NEMO-MED8 model (Sevault et al. 2009) has an implicit free surface option, a buffer zone in the near Atlantic ocean, explicit river runoff fluxes, 43 Z-levels with partial steps and a spatial resolution of 1/8°

(actually from 9 to 12 km from the north to the south of the basin). NEMO-MED8 does not cover the Black Sea (see Figure 1c). Its grid is tilted and stretched within the Gibraltar Strait to increase locally its resolution up to 6 km and to follow better the SW-NE orientation of the strait. The grid definition, the surface forcing method as well as many physical options are the same as in the previous CNRM Mediterranean Sea model (OPAMED8, Somot et al. 2006).

Both ocean models are daily two-way coupled at the Gibraltar Strait and the atmospheric model is daily two-way coupled with both ocean models. The SST of NEMO-MED8 is used over the Mediterranean Sea whereas the SST of NEMO-ORCA2 is used everywhere else. The version 3 of the OASIS coupler developed at CERFACS (Valcke 2006) is used for the air-sea coupling.

The communication between global ocean and Mediterranean Sea is performed as follows: the exchanged fields are temperature and salinity from the global ocean to the Mediterranean Sea and water, heat and salt transports from the Mediterranean Sea to the global ocean.

The near Atlantic of the high resolution Mediterranean Sea model NEMO-MED8 is simulated as an Atlantic box, also called buffer zone in which the 3D temperature and salinity profiles are relaxed towards observed monthly-mean climatology in the stand-alone mode. At the contrary, along the tri-coupled simulation, these profiles are updated every day by the corresponding Atlantic zone of the global ocean model. This allows the NEMO-MED8 model to take into account the daily variability of the near Atlantic surface waters and its likely evolution along the 21st century for example.

From the Mediterranean model to the global ocean, we use the so-called Cross-Land Advection (CLA) parameterization available in NEMO-ORCA2 (Madec 2008, A. Bozec, pers. comm.). The Gibraltar Strait is closed in this low resolution version and the heat, salt and water exchanges through the wall are parameterized. This parameterization allows to assess the MOW characteristics (heat and salt transport) in the Atlantic part of the global model with respect to the characteristics of the Mediterranean deep waters (on the other side of the wall in the stand-alone mode) and of the Atlantic sub-surface waters (entrainment process during the MOW cascading). In the tri-coupled model we replace the low-resolution Mediterranean values by the heat, salt and water transports computed by the high-resolution NEMO-MED8. In the stand-alone mode, the water transports (Gibraltar Inflow, entrainment rate, Atlantic recirculation) are imposed by the CLA. In the tri-coupled model, the Gibraltar inflow is computed by NEMO-MED8, the Gibraltar outflow is computed thanks to the high-resolution MSWB. The only remaining imposed variables are the volume and the depth of the sub-surface entrainment, the Atlantic recirculation at different layers and the depth of the MOW in the Atlantic (1000m). Note that this last and strongest hypothesis is however sustained by a previous Mediterranean Sea climate change scenario (Somot et al. 2006).

The CLA parameterization allows the MOW volume

and hydrological characteristics of the global model to evolve at the daily time-scale depending on NEMO-MED8 evolution.

In the future, a river runoff routing scheme TRIP will be added in this tri-coupled model to simulate the river component of the regional coupled system. The Mediterranean and Black Sea catchment basin is detailed in Figure 2.

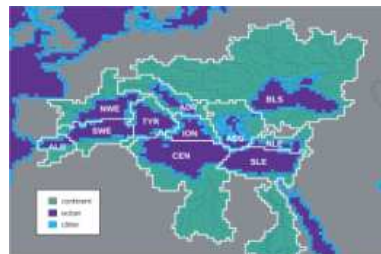


Figure 2: River catchment basin of the Mediterranean Sea (extracted from Ludwig et al. 2009) also used for the TRIP routing scheme model

After spin-up, a first 50-year long simulation using observed GHG and aerosols concentrations has been performed with this Mediterranean tri-coupled AORCM (1950-2000) in the framework of the European CIRCE project. The integrated Mediterranean heat and water (E-P-R) losses are equal to -3.1 W/m^2 and -0.59 m/year in average over 30 years in agreement with current estimates. At the Gibraltar Strait, the surface inflow is equal to 0.78 Sv and the net transport to 0.045 Sv in very good agreement with the latest estimates.

The first scientific goals of such simulation are to study the variability of the Gibraltar Strait exchanges (heat, salt, water transports) and its impact on the variability of the Mediterranean Sea Water Budget and on the variability of the Mediterranean Outflow Waters.

References

1. Déqué M. and Piedelievre J.P. (1995) High-Resolution climate simulation over Europe. *Clim. Dyn.*, 11:321-339
2. Madec G. (2008) NEMO ocean engine, Institut Pierre-Simon Laplace (IPSL), France, Note du pôle de modélisation, 193 pp.
3. Ludwig W., Dumont E., Meybeck M. and Heussner S. (2009) River discharges of water and nutrients to the Mediterranean Sea: Major drivers for ecosystem changes during past and future decades, *Progress In Oceanography*, (accepted)
4. Sevault F., Somot S., Beuvier J. 2009. NEMOMED's user guide. *Note de Centre*, GMGEC (in preparation), available at florence.sevault@meteo.fr (in english)
5. Somot S., Sevault F. and Déqué M., 2006. Transient climate change scenario simulation of the Mediterranean Sea for the 21st century using a high-resolution ocean circulation model. *Clim. Dyn.*, 27(7-8):851-879
6. Somot S. , Sevault F., Déqué M. and Crépon M. (2008) 21st century climate change scenario for the Mediterranean using a coupled Atmosphere-Ocean Regional Climate Model. *Global and Planetary Change*, 63(2-3), pp. 112-126
7. Valcke S. 2006. OASIS3 User Guide (oasis3_prism_2-5). PRISM Support Initiative Report No 3. CERFACS, Toulouse, France. 64 pp.

The Development of Diurnally-Varying Sea-Surface Temperature Scheme.

Part I. Preliminary numerical experiments.

Akiyoshi Wada^{1*} and Yoshimi Kawai²

1) Meteorological Research Institute, Tsukuba, Ibaraki, 305-0052, JAPAN

2) Japan Agency for Marine-Earth Science and Technology, 2-15 Natsushima-Cho, Yokosuka, 237-0061, JAPAN.

*awada@mri-jma.go.jp

1. Introduction

We have developed a new scheme for precisely simulating a diurnally-varying sea-surface temperature (SST). The new scheme is developed to be incorporated into a nonhydrostatic atmosphere model coupled with a slab mixed-layer ocean model (hereafter, the coupled model is referred to as NCM). The new scheme for simulating diurnally-varying SST is formulated based on Schiller and Godfrey (2005) (hereafter referred to as SG). The short-wave absorption/penetration is, however, estimated for the formulation of Ohlmann and Siegel (2000) (hereafter referred to as OG).

2. New scheme

The concept of SG is as follows: A skin layer is formed in the uppermost layer when the short-wave radiation warms the sea surface. The depth of skin layer depends on total short-wave radiation and wind stress accumulated from the sunrise. When a skin layer is thin, the amplitude of diurnally-varying SST is large. After the sunset, the skin layer disappears and the depth of skin layer is equal to the depth of the first, uppermost layer in the ocean model. At that time, total values of short-wave radiation and wind stress have been sustained till the next sunrise.

The formulas associated with short-wave absorption/penetration in OS were derived from the multiple regression analysis. The formulas are functions of chlorophyll concentrations (mg m^{-3}), cloud indices under a cloudy condition and solar zenith angle under a clear-sky condition.

3. Experiment Design

Numerical experiments are performed by the NCM in order to check the performance of new scheme. The integration time is 63 hours. The time step is 10 seconds. The horizontal grid is 32×32 with a grid spacing of 2 km. The short-wave radiation is assumed that the maximum is 1000 W m^{-2} and it is varied with sinusoidal formulas of Danabasoglu et al. (2006). The net flux defined as the summation of upward (from the sea to the surface) long-wave radiation, sensible and latent heat fluxes is set to be 50 W m^{-2} and its value is assumed to be equal to that of latent heat flux. No resultant precipitation occurs during the integration in these experiments. The cloud index is assumed to zero for the numerical experiments. The value of chlorophyll concentration is assumed to be 0.1 and 1 mg m^{-3} and has not been changed during the integration. The depth of the first, uppermost layer (hereafter referred to as dz) is set to be 5 m. Wind stresses are derived from wind speeds at the first, lowermost layer in the atmospheric part of NCM and bulk formula of Kondo (1975) incorporated into the atmospheric part of NCM.

4. Results

Figure 1 indicates the evolution of skin layer depth ($zD_s(t)$) diagnosed by the new scheme. The time '0' indicates the initial time at 0000 UTC (0900 JST). When the numerical experiments are initiated to run, $zD_s(t)$ turns to be thin around 0100 UTC (1000JST). After that, $zD_s(t)$ becomes thicker. After the sunset, high wind speed leads to thick $zD_s(t)$, which is equal to dz at the maximum. Figure 1 also indicates that $zD_s(t)$ becomes

thin as the wind speed is low. Low wind speed is also associated with the sustenance of thin depth of $z_{D_i}(t)$ after the sunset.

Figure 2 indicates the evolution of SST simulated by the NCM with the new scheme. The chlorophyll concentration is 0.1 mg m^{-3} . The simulated SST shows diurnal variations. Without the new scheme, the amplitude of diurnally-varying SST is small, while the new scheme produces larger amplitude of diurnally-varying SST. An increase in the peak SST is nearly 0.5°C when the wind speed is 3.0 m s^{-1} .

Figure 3 indicates the evolution of SST simulated by the NCM with the new scheme except that the chlorophyll concentration is 1 mg m^{-3} . The peak amplitude of simulated SST increases by 0.1° compared with that shown in Fig. 2. This suggests that high chlorophyll concentration leads to large amplitude of diurnally-varying SST. This is due to high absorption of solar radiation near the sea surface.

Because this paper describes only the performance of new scheme in the ocean part of NCM, the impact of diurnally-varying SST on the atmosphere is beyond the scope of this paper. However, net flux is affected by the variation of SST. In addition, wind stress may be affected by the variation of SST, indicating that the variation of wind stress can affect the variation of SST in turn. This issue is reported by Wada and Kawai (2009) in this Blue Book (2009).

References

- Danabasoglu, G., W.G. Large, J.J. Tribbia, P.R. Gent, B.P. Briegleb, and J.C. McWilliams, 2006: Diurnal Coupling in the Tropical Oceans of CCSM3. *J. Climate*, 19, 2347–2365.
- Kondo, J., 1975: Air-sea bulk transfer coefficients in diabatic conditions. *Bound.-Layer Meteor.*, 9, 91-112.
- Ohlmann, J.C., and D.A. Siegel, 2000: Ocean Radiant Heating. Part II: Parameterizing Solar Radiation Transmission through the Upper Ocean. *J. Phys. Oceanogr.*, 30, 1849–1865.
- Schiller, A., and J. S. Godfrey, 2005: A diagnostic model of the diurnal cycle of sea surface temperature for use in coupled ocean-atmosphere models. *J. Geophys. Res.*, 110, C11014, doi:10.1029/2005JC002975.
- Wada, A., and Y. Kawai, 2009: The development of diurnally-varying sea-surface temperature scheme. Part II. Idealized numerical experiments. CAS/JSC WGNE Research Activities in Atmosphere and Oceanic Modelling, Submitted.

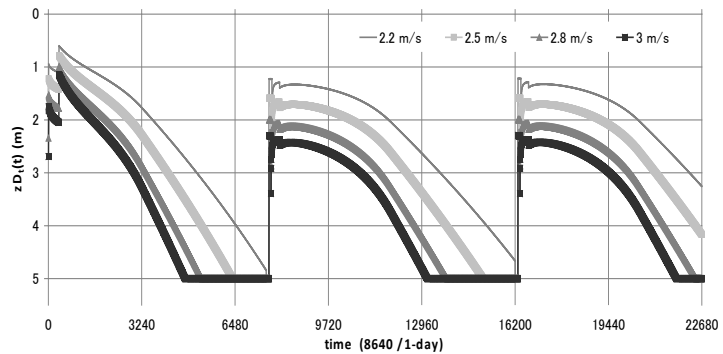


Figure 1 The evolution of skin layer depth ($z_{D_i}(t)$) diagnosed by the new scheme

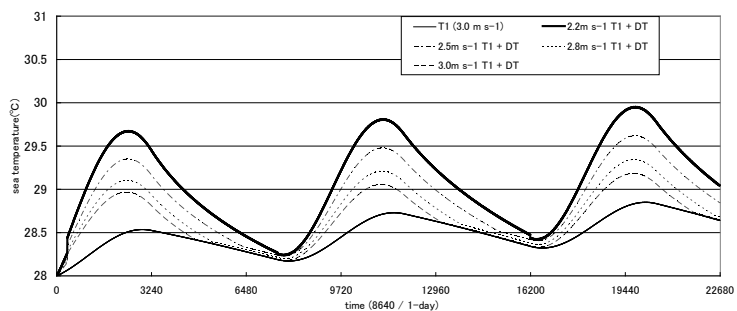


Figure 2 The evolution of SST simulated by the new scheme. A chlorophyll concentration is 0.1 mg m^{-3} .

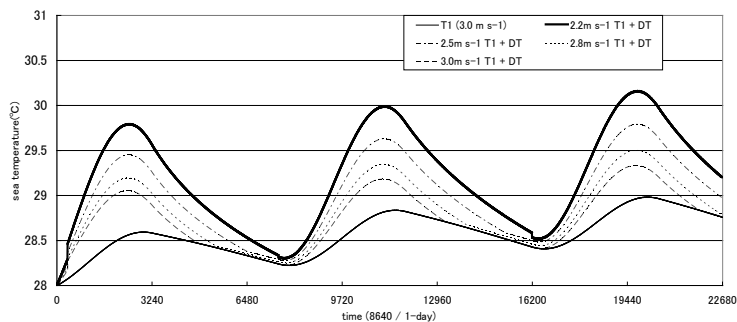


Figure 3 As in Fig. 2 except that a chlorophyll concentration is 1 mg m^{-3} .

This work was supported by Japan Society for the Promotion of Science (JSPS), Grant-in-Aid for Scientific Research (C) (19612005).

The Development of Diurnally-Varying Sea-Surface Temperature Scheme. Part II. Idealized numerical experiments.

Akiyoshi Wada ^{1*} and Yoshimi Kawai ²

1) Meteorological Research Institute, Tsukuba, Ibaraki, 305-0052, JAPAN

2) Japan Agency for Marine-Earth Science and Technology, 2-15 Natsushima-Cho, Yokosuka, 237-0061, JAPAN.

*awada@mri-jma.go.jp

1. Introduction

We have developed a new scheme for precisely simulating a diurnally-varying sea-surface temperature (SST) (Wada and Kawai, 2009). In this paper, new scheme based on Schiller and Godfrey (2005) (hereafter referred to as SG) is incorporated into a nonhydrostatic atmosphere model coupled with a slab mixed-layer ocean model (hereafter NCM). In order to investigate the impact of diurnally-varying SST on the atmosphere, idealized numerical experiments were performed by the NCM.

2. Experiment Design

In order to perform the numerical experiments by the NCM, atmospheric and oceanic initial conditions are required. The atmospheric initial condition is provided from the Japan Meteorological Agency Regional Analysis data. The atmospheric profile is assumed to be uniform with the reference to the profile around 139°E, 29.5°N at 0000 UTC (0900 JST) on 27 June in 2004. The initial sea temperatures are 28 °C at the sea surface (SST), 27 °C at the mixed-layer base, 15 °C at the thermocline base and 5 °C at the bottom level. Salinity is assumed to be homogeneously 35. Layer thicknesses are 5 m in the mixed layer, 45 m in the thermocline, 450 m in the lowermost layer. The Coriolis parameter is 5×10^{-5} .

The integration time is 288 hours. During the integration from the initial time to 48h, the numerical experiments were performed by the nonhydrostatic atmosphere model (NHM). After 48 hours, the numerical experiments were performed by the NHM and the NCM. The time step is 10 seconds. The horizontal-grid number is 32 x 32 with the grid spacing of 2 km. The number of vertical layer is 40. The interval of vertical layers is changed from 40 m (near the surface) to 1180m (upper atmosphere). The top height is nearly 23 km.

In SG, solar radiation, cloud index and wind stress are provided by the NCM. The value of chlorophyll concentration is assumed to be 0.1 and 1 mg m⁻³ and has not been changed during the integration. The depth of uppermost layer (hereafter referred to as dz) is set to be 5 m, which is equal to the mixed-layer depth at the initial time in NCM. In order to investigate the impact of solar radiation on the skin-depth (hereafter zDt) and the amplitude of computed SST, sensitivity experiments are preformed: Solar radiation (Wind stress) is 1.5 (0.75) times larger than that of control experiments (CNTL). The specification and abbreviation of numerical experiments are listed in Table 1.

Table 1 Specification of numerical experiments

	Atmospheric forcing
CNTL	From regional analysis data
SR15	Solar radiation is 1.5 times only in SG
WD075	Wind stress is 0.75 times only in SG
SRWD	Solar radiation is 1.5 times and Wind stress is 0.75 times only in SG

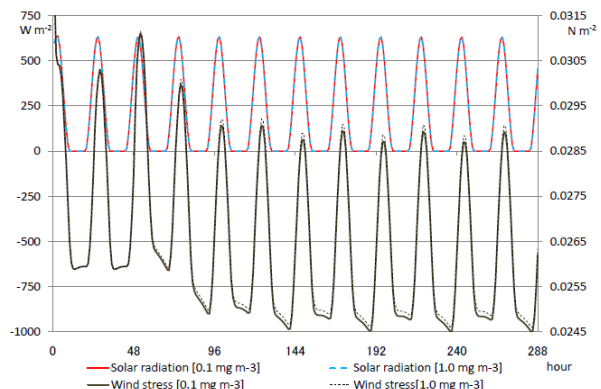


Figure 1 Time series of solar radiation and wind stress in CNTL (0.1 mg m⁻³) and CNTL (1.0 mg m⁻³). Each figure enclosed within parentheses indicates a chlorophyll concentration.

3. Results

3.1 Short-wave radiation and wind stress

Figure 1 depicts the time series of solar radiation and wind stress in CNTL (0.1 mg m⁻³) and CNTL (1.0 mg m⁻³). Solar radiation varies diurnally, while computed wind stress varies with a period of two days. The computed wind stress is reduced after NCM begins to run. A difference in solar radiation is not seen between CNTL (0.1 mg m⁻³) and CNTL (1.0 mg m⁻³). On the other hand, a difference in wind stress can be seen when solar radiation is nearly zero in a day.

3.2 Depth of skin layer and simulated SST

Figure 2 depicts the time series of zDt and SST in CNTL (0.1 mg m⁻³) and CNTL (1.0 mg m⁻³). After the sunrise (around 0100-0200 UTC), zDt becomes small but turns to the value of dz. This recovery of zDt is probably due to relatively small solar radiation and strong wind stress. This is the reason why a difference in zDt is not seen between CNTL (0.1 mg m⁻³) and CNTL (1.0 mg m⁻³). A difference in SST between CNTL (0.1 mg m⁻³) and CNTL (1.0 mg m⁻³) is at most 0.1 °C. The amplitude of diurnally-varying SST is large when a chlorophyll concentration is high.

3.3 The impact of solar radiation

Figure 3a depicts the time series of SST and zDt in CNTL, SR15, WD075 and SRWD when the chlorophyll concentration is 0.1 mg m⁻³. A difference in SST is not seen except for the SRWD. The period of shallow zDt is only three-four hours in WD075 and only 1-hour in CNTL. The period of shallow zDt in SRWD is longest in four experiments. This suggests that this scheme is sensitive only to extremely high solar radiation and extremely weak wind stress, or both conditions are needed to compute apparent peak of diurnally-varying SST. Figure 3b depicts the time series of wind stress at the lowermost, first layer. When zDt becomes shallow and SST within the depth of zDt increases, wind stress is slightly stronger. In addition, wind stress is stronger during the night even though zDt is 5 m. This suggests that a peak of SST leads to the enhancement of wind stress during the night. It should be noted that a 2-day period is seen in the evolution of wind stress. Enhanced wind stress suppresses the amplitude of diurnally-varying SST in turn and then weakens the wind stress in the next day.

References

- Wada, A. and Y. Kawai, 2009: The development of diurnally-varying sea-surface temperature scheme. Part I. Preliminary numerical experiments. CAS/JSC WGNE Research Activities in Atmosphere and Oceanic Modelling, Submitted.
- Schiller, A., and J. S. Godfrey, 2005: A diagnostic model of the diurnal cycle of sea surface temperature for use in coupled ocean-atmosphere models, J. Geophys. Res., 110, C11014, doi:10.1029/2005JC002975.

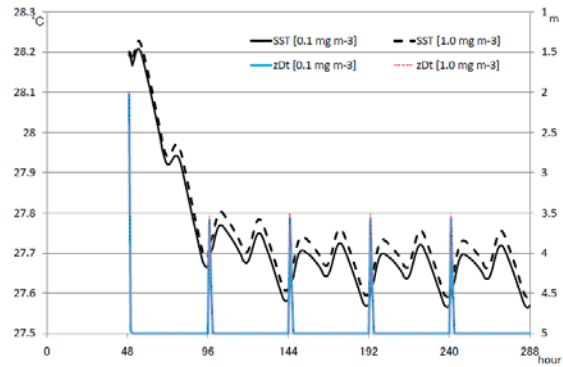


Figure 2 Time series of zDt and SST in CNTL (0.1 mg m⁻³) and CNTL (1.0 mg m⁻³). Each figure enclosed within parentheses is the same as figure 1

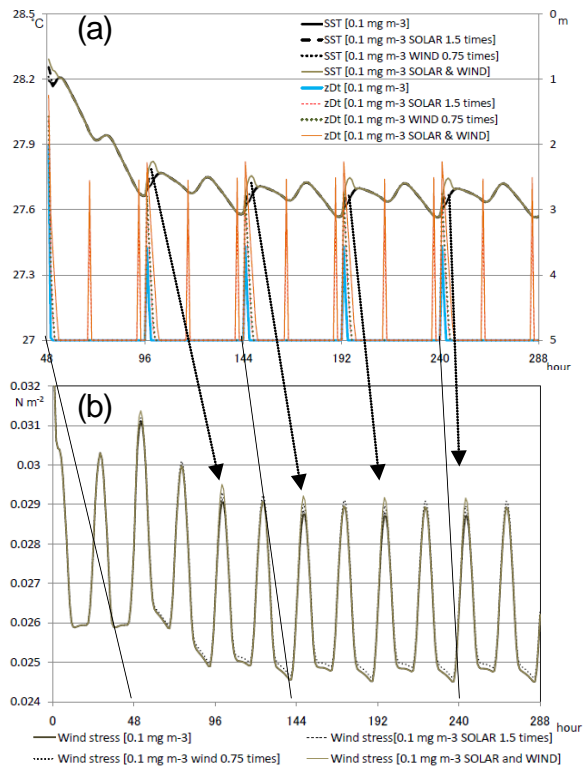


Figure 3 (a) As Fig. 1 except for CNTL (0.1 mg m⁻³), SR15 (0.1 mg m⁻³) and WD075 (0.1 mg m⁻³). (b) As Fig. 2 except for CNTL (0.1 mg m⁻³), SR15 (0.1 mg m⁻³) and WD075 (0.1 mg m⁻³).

This work was supported by Japan Society for the Promotion of Science (JSPS), Grant-in-Aid for Scientific Research (C) (19612005).

Numerical predictions for Typhoon Hai-Tang in 2005 by an experimental atmosphere-wave-ocean coupled model

Akiyoshi Wada^{1*}, Nadao Kohno² and Norihisa Usui¹

1) Meteorological Research Institute, Tsukuba, Ibaraki, 305-0052, JAPAN

2) Japan Meteorological Agency, Chiyoda, Tokyo, 100-8122, JAPAN

*awada@mri-jma.go.jp

1. Introduction

The predictions of typhoons have been improved for a decade particularly in their track predictions due to the developments of numerical modeling, assimilation and observational technologies. However, their intensity predictions have been still less precise compared with their track predictions. In order to improve the intensity predictions, we need to develop a regional atmosphere-wave-ocean coupled model. The reason for it is that sea-surface cooling (SSC) affects the typhoon intensity predictions directly, while ocean wave affects the structure of typhoon (Kohno and Murata, 2007). In this paper, we have developed a regional atmosphere-wave-ocean coupled model for improving the typhoon intensity predictions and perform numerical predictions for Typhoon Hai-Tang in 2005 using an experimental atmosphere-wave-ocean coupled model.

2. Coupled model

The coupled model consists of nonhydrostatic atmospheric model (NHM), Meteorological Research Institute (MRI) the third generation ocean wave model (MRI-III) and slab mixed-layer ocean model (MLOM). Figure 1 depicts a schematic diagram associated with exchange processes among NHM, MRI-III, and MLOM. Even though various expressions are proposed (Kohno and Murata, 2007), the formula in Taylor and Yelland (2001) is used as the roughness expression.

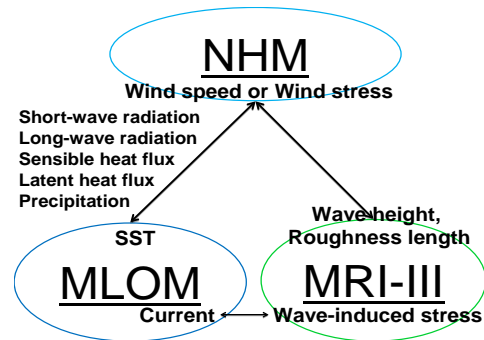


Figure 1 Schematic diagram of exchange processes among NHM, MRI-III and MLOM.

3. Experiment Design

The horizontal grid is 721 x 421 with the grid spacing of 6 km and 1441 x 841 with that of 3 km. The number of vertical layer is 40. The interval of vertical layers is changed from 40 m (near the surface) to 1180 m (upper atmosphere). The top height is nearly 23 km. Cumulus parameterization (Kain and Fritsch, 1990, hereafter KF) is used for simulating sub-grid-scale cumulus convection when numerical predictions are performed by NHM with horizontal-grid spacing of 6 km. A diurnally-varying sea-surface temperature (SST) scheme (Wada and Kawai, 2009) is introduced to the MLOM. The number of layer in MLOM is three (mixed-layer, thermocline and the bottom layer). The depth at the thermocline depth is 600 m and that at the bottom is 2000m at the deepest bottom. The mixed-layer depth is determined from daily oceanic reanalysis data as the depth at which the difference in density is within 0.25 kg m^{-3} from the surface.

The initial and boundary conditions are obtained from the results of numerical simulations by the global spectral model (GSM) and typhoon model (TYM). The resolution version of GSM is T213L40. The horizontal resolution of TYM is nearly 20 km near the center of typhoon. The integration times of both GSM and TYM are 72 hours.

Numerical predictions were performed for Typhoon Hai-Tang in 2005 by an experimental atmosphere-wave-ocean coupled model. The initial time in GSM, TYM and the coupled model is at 1200 UTC on 12 July in 2005. Typhoon bogus has been embedded when the TYM was initiated to run. We used daily SST data as the initial condition in the runs by the GSM and TYM. On the other hand, daily oceanic reanalysis data provided from an ocean data assimilation system were used for the run by the coupled model. Two runs were performed by the coupled model with horizontal-grid spacing of 6 km and with different oceanic preconditions: daily reanalysis temperature and salinity on 12 July in 2005 (hereafter Ex05) year and in 1999 (hereafter Ex99) year. In addition, preliminary numerical predictions by the coupled model with horizontal-grid spacing of 3km were performed by the coupled model only in EX05.

4. Results

Figure 2 plots the results of track predictions by the atmosphere-wave-ocean coupled model (corresponding to 'Wave' in Fig. 3, hereafter Wave) in Ex05 (6 km) and Ex99 (6 km). The best track indicates southwestward translation at the early integration and then westward/west-northwestward translation. The best-track central pressure (CP) reaches 940 hPa during the rapid intensification phase (Fig. 3). Predicted tracks in Ex05 (6 km) and Ex99 (6 km) indicate west-northwestward translation at 0000 UTC on 13 July and then southwestward translation (Fig.2).

CPs by NHM ('Atmos' in Fig. 3, hereafter Atmos) are relatively lower than those in best-track data. On the other hand, CPs by Wave and atmosphere-ocean ('Ocean' in Fig. 3, hereafter Ocean) coupled models in Ex05 (6 km) and Ex99 (6 km) are higher than those in best-track data after 23h. Particularly, predicted CPs hardly change from 12h to 36h and from 48h to 60h when Hai-tang's best track CP shows rapid intensification. After 60h, we can find that Hai-Tang's intensification is well simulated in Atmos, Ocean and Wave. Figure 3 also suggests that the negative feedback is affected by the oceanic precondition represented by its difference between Ex05 (6 km) and Ex99 (6 km). However, it should be noted that a difference in predicted CPs is at most 5 hPa.

Because KF is used as cumulus parameterization in both Ex05 (6 km) and Ex99 (6 km), we performed additional numerical predictions using the models with horizontal-grid spacing of 3km (Ex05 (3km)). The tendency of CPs in Figure 4 is similar to that in Figure 3. At 48h, the value of CP in Wave is 975.7 hPa, that in Ocean is 981.3 hPa and that in Atmos is 942.3 hPa. On the other hand, that in Wave (3km) is 976.8 hPa, that in Ocean (3km) is 979.6 hPa and that in Atmos (3km) is 941.3 hPa. The results suggest that finer horizontal resolution hardly contributes to the improvement of intensity prediction. The effect of lack of KF parameterization on CP may balance with that of the change of resolution from 6 km to 3 km on CP.

The reason for high CPs in Ocean and WAVE is that the impact of entrainment estimated by modified Deardorff formulation (Wada et al, 2009) on Hai-Tang-induced SSC is so strong that Hai-Tang hardly intensifies. The tuning parameters ($m = 175$ and $\alpha=5$) in modified Deardorff formulation should be determined based on atmospheric forcings. In the future, we will check these parameters, perform more additional numerical predictions and then investigate the rapid-intensification process.

References

- Kain, J.S., and J.M. Fritsch, 1990: A One-Dimensional Entraining/Detraining Plume Model and Its Application in Convective Parameterization. *J. Atmos. Sci.*, 47, 2784–2802.
- Kohno, N. and A. Murata, 2007: The Impact of the Sea State on the Typhoon Intensity in Atmosphere-wave coupled model. *CAS/JSC WGNE Research Activities in Atmosphere and Oceanic Modelling*, 4-13.
- Taylor, P. K. and M. J. Yelland, 2001: The dependence of sea surface roughness on the height and steepness of the waves. *J. Phys. Oceanogr.*, 31, 572-590.
- Wada, A. and Y. Kawai, 2009a: The Development of Diurnally-Varying Sea Surface Temperature Scheme. Part I. Preliminary experiments. *CAS/JSC WGNE Research Activities in Atmosphere and Oceanic Modelling*, Submitted.
- Wada, A., H. Niino and H. Nakano, 2009: Roles of Vertical Turbulent Mixing in the Ocean Response to Typhoon Rex (1998), *J. Oceanogr.* Accepted.

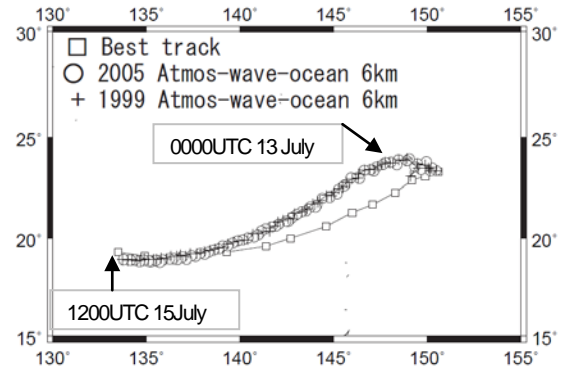


Figure 2 Results of track predictions. Squares show typhoon positions from JMA best track. Circles show those from the prediction with the initial ocean condition in 2005. Plus marks show those with the initial ocean condition in 1999.

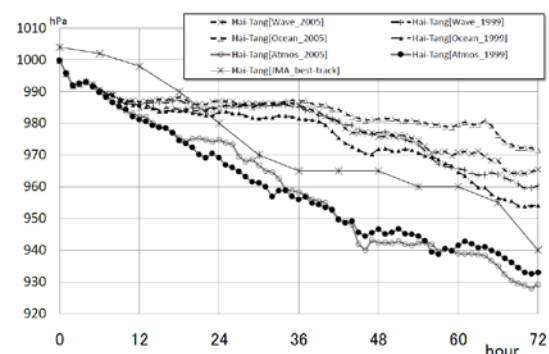


Figure 3 Evolution of best-track and predicted central pressure by models with horizontal-grid spacing of 6km and KF parameterizations. Asterisks show central pressure from JMA best track.

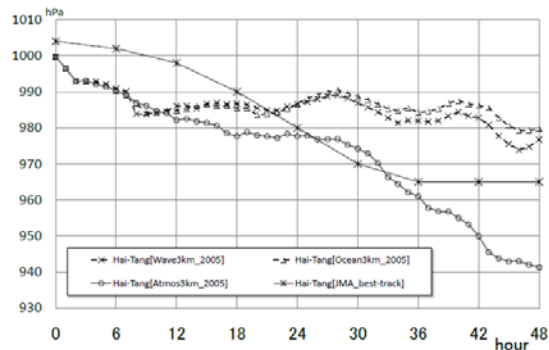


Figure 4 Same as Figure 3 except for the evolution by models with horizontal-grid spacing of 3 km and without KF parameterization.

The Impacts of an Active Ocean Boundary Condition on Tropical Cyclone Evolution Using a Coupled Atmosphere-Ocean Model

Henry R. Winterbottom¹ and Eric P. Chassignet

*Center for Ocean-Atmosphere Prediction Studies, The Florida State University
Tallahassee, FL 32306, USA*

1. Introduction

In response to the need to improve the understanding of tropical cyclones (TC), especially in the wake of recent events such as Charley (2004) and Katrina (2005), much effort has been invested towards improving the Numerical Weather Prediction (NWP) model's ability to forecast the track, intensity, and structure of TCs. Presently, NWP models are employed by both the operational meteorological centers and research institutions where scientists are attempting to understand the factors which modulate the tendencies in a respective TC's track, structure, and intensity. The National Hurricane Center (NHC), in Miami, FL, reports that considerable improvements in track forecast skill has been attained, partly as a result of the evolution of NWP. However, there remains considerably less skill when attempting to forecast a TC's intensity.

One of the suggested hypotheses to explain the inability of NWP to improve intensity forecasts is that many models *ignore* the evolution of the ocean sea-surface temperature (SST) during the TC passage. As a result, the air-sea interactions and resultant fluxes, which are linked to the upwelling and cooling of the SST, are not resolved, and can subsequently have unrealistic impacts on the structure and intensity for the TC (Price, 1981; Brooks, 1983; Bender and Ginis, 2000; Shay et al., 2000; Chan et al., 2001). In this discussion, we illustrate the current stages in the development of a coupled atmosphere-ocean model which will be used to better understand and address the deficiencies related to forecasting TC intensity – particularly as the pertain to air-sea interactions. In the following section, we provide a brief description of the coupled-modeling system, which is followed by the results of a simple twin-experiment for TC Bertha (2008). Finally, we conclude with the future work regarding this subject.

2. Model Configuration and Initial Experiments

The atmospheric model in the coupled-model system is the **Weather Research and Forecasting (WRF) Advanced Research WRF (ARW)** (Skamarock et al., 2005). The ocean model for the coupled-model system is the **HYbrid Coordinate Ocean Model (HYCOM)** (Bleck, 2002; Chassignet et al., 2003; Halliwell, 2004). The equatorial resolution for the HYCOM grid is $1/12^\circ$ and is a sub-region of the NAVO²/NRL³ global HYCOM (Wallcraft et al., 2005). The WRF-ARW grid is defined using a Mercator projection with a grid-length resolution of approximately 8.81-km. The WRF-ARW grid resolution is chosen so as to co-locate the HYCOM and WRF-ARW grids as closely as possible. The initial and boundary conditions are obtained from the NAVO/NRL Global HYCOM analysis grids and the NCEP⁴ 1.0° FNL analysis. The HYCOM model grid has $X \times Y \times Z$ dimension $1063 \times 545 \times 32$ while the WRF-ARW grid dimension is $1083 \times 565 \times 35$.

The coupling procedure is as follows: (1) The atmosphere model (WRF-ARW) integrates from $t=0$ to $t=dt$ – where dt is the coupling interval, to calculate all the atmospheric forcing variables that are required to force the ocean model (HYCOM). (2) The WRF-ARW forcing variables for 10-meter wind (U), zonal- and meridional wind stress (τ_x and τ_y), 2-meter temperature (T_2) and specific humidity (q_2), precipitation rate (\dot{R}), and the net downward (into the ocean) long- and short-wave radiation fluxes (Q_{LW} and Q_{SW} , respectively) are calculated and interpolated to the ocean model grid. (3) HYCOM integrates from $t=0$ to $t=dt$ and calculates a sea-surface temperature (SST) grid defined by the prescribed WRF-ARW forcing. (4) The HYCOM SST is interpolated to the WRF-ARW grid and updated within the boundary condition file. This coupling cycle repeats at the interval of dt and continues for the duration of the forecast.

Fig. 1 illustrates the 72-hour forecast (initialized 00Z 11 July) latent-heat flux (LHF) swath for TC Bertha (2008). The un-coupled model simulation is one in which the SST is held fixed for the duration of the forecast, while the coupled forecast is one in which the atmosphere and ocean interact along each hour. The coupling interval is chosen to illustrate the differences between the un-coupled and coupled model simulations. The differences in the LHF values, namely the lower maximum values for the coupled-model, suggest that the air-sea interactions act to modulate the intensity of the TC. Fig. 2 illustrates the log-scale normalized minimum sea-level pressure (MSLP) time-series for the respective TC Bertha (2008) simulations and the best-track re-analysis (BTRA). It is clear that the air-sea interactions, which are afforded by the coupled-model, have a dramatic impact on the intensity of the TC and that the intensity modulations, relative to the BTRA, are better represented.

¹Corresponding Author: hwinter@met.fsu.edu

²NAVval Oceanographic Office, Stennis Space Center, MS, USA

³Naval Research Laboratory, Stennis Space Center, MS, USA

⁴National Center for Environmental Prediction, Camp Springs, MD, USA

3. Ongoing and Future Developments

The configuration described within this document produces near real-time forecasts for the atmospheric and oceanic variables currently believed to enable forecaster’s to understand the genesis and life-cycle aspects, as well as the synoptic-scale interactions for TCs. The forecasts produced by the respective atmosphere (WRF-ARW⁵) and ocean (HYCOM⁶) models can be viewed online.

These preliminary results, illustrating the impacts upon TC vortex, suggest that the coupled-model is performing satisfactorily. However, as with all NWP problems, the quality of the model solution is highly sensitive to the initial conditions provided to the model. It is worth noting that the initial conditions for the atmospheric model (ie. the TC vortex structure) are considerably different in terms of both the structure and intensity relative to the available observations. Though the intensity modulations for the coupled-model simulation and the BTRA are similar, the MSLP intensities calculated by the coupled-model indicate a considerably weaker TC than those contained in the BTRA. This suggests, that in order to fully understand and realize both the temporal and spatial scales of the air-sea interaction dynamics, an improved initial state pertaining to the vortex structure, intensity, and position is desired. The implementation of a vortex specification scheme, akin to the GFDL⁷ method (Kurihara et al., 1995), as well as the incorporation of a wave-model parameterization within the coupled-model system are the next features to be included. The vortex initialization will use observed 2-D surface wind analyses, while the wave-model will include wind-stress parameterizations which have been derived from observations collected within high-wind speed events. The uses of both an improved initial vortex state and parameterizations derived within TC-type environments will lead to further improvements in the model’s representation of the sea-state as well as a better representation of the enthalpy exchanges associated with the sea-spray and moisture fluxes from the ocean into the atmospheric boundary-layer.

4. References

Bender, M.A., and I. Ginis, 2000: Real-Case Simulations of Hurricane Ocean Interaction Using A High-Resolution Coupled Model: Effects on Hurricane Intensity. *Mon. Wea. Rev.*, **128**, 917-946.

Bleck, R., 2002: An oceanic general circulation model framed in hybrid isopycnic-cartesian coordinates. *Ocean Modeling*, **4**, 55–88.

Brooks, D.A., 1983: The Wake of Hurricane Allen in the Western Gulf of Mexico. *J. Phys. Oceanogr.*, **13**, 117-129.

Chan, J.C.L., Y. Duan, and L.K. Shay, 2001: Tropical Cyclone Intensity Change from a Simple Ocean Atmosphere Coupled Model. *J. Atmos. Sci.*, **58**, 154-172.

Chassignet, E.P., L.T. Smith, G.R. Halliwell, and R. Bleck, 2003: North Atlantic simulation with the HYbrid Coordinate Ocean Model (HYCOM): Impact of the vertical coordinate choice, reference density, and thermobaricity. *J. Phys. Oceanogr.*, **33**, 2504–2526.

Halliwell, G.R., 2004: Evaluation of vertical coordinate and vertical mixing algorithms in the HYbrid Coordinate Ocean Model (HYCOM). *Ocean Modeling*, **7**, 285–322.

Kurihara, Y., M.A. Bender, R.E. Tuleya, and R.J. Ross, 1995: Improvements in the GFDL Hurricane Prediction System. *Mon. Wea. Rev.*, **123**, 2791–2801.

Price, J.F., 1981: Upper Ocean Response to a Hurricane. *J. Phys. Oceanogr.*, **11**, 153-175.

Shay, L.K., G.J. Goni, and P.G. Black, 2000: Effects of a Warm Oceanic Feature on Hurricane Opal. *Mon. Wea. Rev.*, **128**, 1366-1383.

Skamarock, W.C., J.B. Klemp, J. Dudhia, D.O. Gill, D.M. Barker, W. Wang, and J.G. Powers, 2005: A description of the Advanced Research WRF Version 2. NCAR Tech Notes-468+STR.

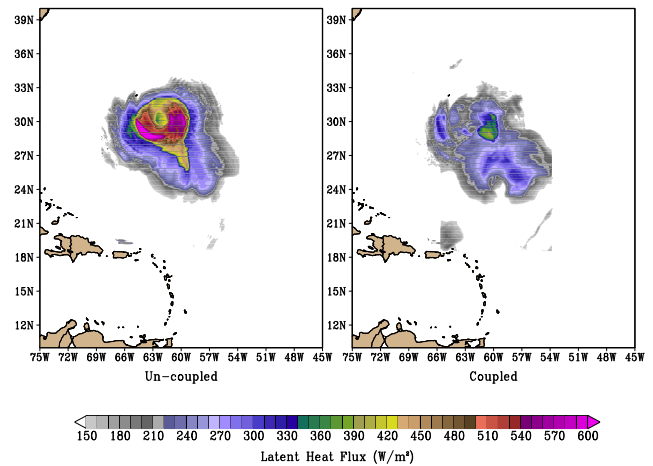


Fig. 1: Latent-heat flux swaths for TC Bertha (2008), initialized 00Z 11 July, for an un-coupled (left) and coupled (right) model simulation.

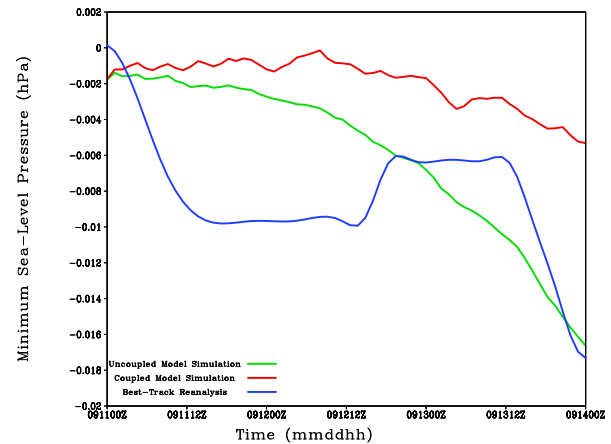


Fig. 2: Normalized and log-scaled MSLP time-series for the un-coupled (green) and coupled (red) model simulations, as well as the BTRA (blue) for TC Bertha (2008). Time-series spans from 00Z 11 July thru 00Z 14 July.

⁵<http://www.coaps.fsu.edu/~hwinter/wrfarwtc>

⁶<http://www.coaps.fsu.edu/~hwinter/hycomtc>

⁷Geophysical Fluid Dynamics Laboratory, Princeton, NJ, USA